# Wind forced currents over the shallow Naissaar Bank in the Gulf of Finland

## Madis-Jaak Lilover, Juss Pavelson and Tarmo Kõuts

*Marine Systems Institute at Tallinn University of Technology, Akadeemia tee 21, EE-12618 Tallinn, Estonia*

Lilover, M.-J., Pavelson, J. & Kõuts, T. 2011: Wind forced currents over the shallow Naissaar Bank in the Gulf of Finland. *Boreal Env. Res.* 16 (suppl. A): 164–174.

We performed current velocity observations on Naissaar Bank in northern Tallinn Bay, Gulf of Finland, for five weeks in late autumn 2008 using a bottom-mounted ADCP deployed at 8 m depth. Strong and variable, mainly southerly winds with speeds exceeding 10 m s$^{-1}$ dominated in the area during 60% of the whole period. Bursts of seiche-driven currents with periods of 31, 24, 19.5, 16 and 11 h were observed after the passage of wind fronts. Inertial oscillations and diurnal tidal currents were relatively weak. The low-frequency current velocities gradually decreased toward the bottom at 3 cm s$^{-1}$ over 4-m distance. The magnitude of the complex correlation coefficient between the current and wind for the whole series was 0.69, but it was much higher (up to 0.90) within the shorter steady wind periods. The current was rotated ~35° to the right from the wind. As an exception, during one period a counterclockwise surface-to-bottom veering of the current vector was observed. A topographically steered flow was seen either along isobaths of the bank during strong winds or along the 'channel' at the entrance to Tallinn Bay.

## Introduction

The Gulf of Finland is an elongated estuarine-like sub-basin of the Baltic Sea with a complicated dynamic activity. The main preconditions for the development of dynamic processes of different scale are the variable coastline and bottom topography of the gulf, the changing wind field over the gulf promoted by the mostly eastward moving atmospheric cyclones and the large freshwater inflow of the Neva River at the eastern end of the gulf. In the last decade, the circulation pattern in the gulf was relatively well reproduced by numerical models (e.g., Andrejev *et al.* 2004, Zhurbas *et al.* 2008). Unfortunately, there is still a shortage of current measurements in the area. Historical observations with reference to the cyclonic nature of surface circulation in the gulf were thoroughly reviewed by Alenius *et al.* (1998). The latest reported measurements with the aim to study various mesoscale processes in the coastal areas of the gulf were performed by means of acoustic profilers, ship-mounted ADCP (Raudsepp 1998, Laanemets *et al.* 2005) as well as bottom-mounted ADCP (Suursaar and Aps 2007).

In the present study, we focus on the response of currents (measured by a bottom-mounted ADCP) over the shallow Naissaar Bank to varying winds. In the Gulf of Finland the varying winds were found to give rise to considerable variations of wind-driven currents (Alenius *et al.*

1998, Gästgifvars *et al*. 2006), to cause upwellings/downwellings with related jets (Talpsepp *et al*. 1994, Laanemets *et al*. 2005) as well as to modify the local geostrophic balance in the upper mixed layer (Raudsepp 1998). Moreover, inertial oscillations and seiches with accompanying currents are usually generated after the passage of wind fronts (Alenius *et al*. 1998 and references therein). Considering our observation site on the top of a bank surrounded by neighboring banks at the entrance to a smaller bay (Fig. 1), the resulting near-surface currents will presumably be rather complicated.

To explain different features of the current field, the Ekman theory, based on the balance of the frictional and the Coriolis forces, is widely used in physical oceanography. At our measurement site the surface and bottom boundary layers probably overlapped, i.e. there was most likely an interaction between the two layers. Generally, in a shallow sea the effect of the Coriolis force becomes less important due to the increased bottom friction and therefore, the spirals of both layers tend to cancel each other. Thus, the current over our very shallow site expectedly aligns with the wind direction. However, the interaction of the layers together with the effect of the surrounding bottom topography should strongly modify the current behavior. The current measurements in shallow water in earlier studies with the bottom depth comparable to that at our site were performed mainly in either the inner shelf of an ocean (e.g., Lentz *et al*. 2008) or in the coastal zone of semi-enclosed seas (e.g., Lass *et al*. 2001). These studies exposed vertically sheared currents in accordance with the Ekman model, but the background conditions (location relative to the coast and vertical stratification) were different from our study.

The main objective of this study is to analyze the response of the currents to highly variable winds. For this purpose we first shortly describe the wind and current velocity series and determine and explain the most energetic submesoscale harmonic oscillations of the currents using the spectral analysis. After removing these oscillations from the series, we estimate the correlation between the wind and current residual vectors as well as the effect of the local bottom topography on the residual current.
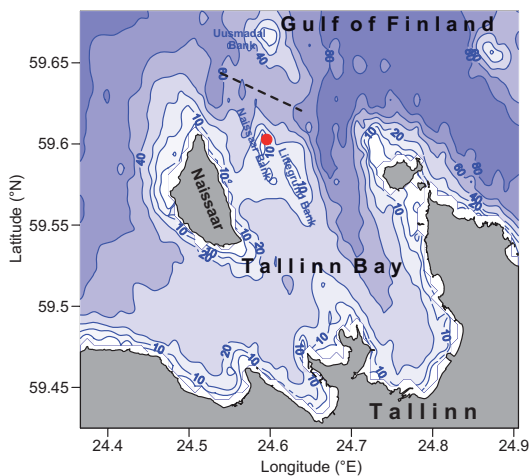


**Fig. 1**. Map of Tallinn Bay with bathymetry. The red circle shows the location of the bottom-mounted ADCP. The axis of the channel between Naissaar Bank and Uusmadal Bank is shown by the dashed line.

## Material and methods

The current velocity measurements were carried out on Naissaar Bank in the northern part of Tallinn Bay (Fig. 1) in the central Gulf of Finland. The dimensions of this water body are about 10 × 15 km. A relatively deep trench extending far into the bay changes to a shallower area composed of several banks toward the E and NE of the island of Naissaar. Our observation site was located near the northern tip (59°35.8′N, 24°35.8′E) of Naissaar Bank. The NNW–SSE oriented bank is about 4 km long, 1.5 km wide and in places 5 m deep. We used a 307.2 kHz broad-band ADCP (RDInstruments) deployed on the bottom at 8 m depth with a trawl-resistant platform Barnacle 60P from 30 October to 6 December 2008. The instrument measured velocities in the depth range of 0–5 m over 0.5 m bins with the sampling interval of 10 min (average of 50 pings). The water temperature as an ancillary parameter was measured at about 0.6 m above the bottom. Sea level data from Tallinn and Sillamäe (170 km to the east from Tallinn) gauges were used for some interpretations. A wave gauge was also deployed at the site, but because of its serious malfunctioning the wave data were not usable.

The uppermost bin (0–0.5 m) was removed from the ADCP data set as contaminated by the

surface side lobe effect. The quality of the data at each depth bin was checked using the procedure developed by Book *et al.* (2007), which is based on the error velocity statistics and on certain criteria for the other internal control parameters (percentage good, signal correlation) of the ADCP. Relying on this analysis, the data from the second bin from the surface (0.5–1 m depth) were also removed from the data set. High-resolution wind data for this period were available from the Tallinnamadal Lighthouse (59°42.7′N, 24°43.9′E) located 15 km toward the NE of our measurement site. The wind speed and direction sensors (Aanderaa) were located at the height of 31 m and the data were recorded every 5 min. The wind data were not converted into the standard 10-m height level because of the uncertainty of the vertical stratification conditions. Considering the atmospheric stratification type, the wind speed reduction factor for our data should be in the range 0.74–0.91 (Launiainen and Laurila 1984).

We applied the following methods to analyze the current and wind vector series. The velocity vector for a specified frequency band was separated into clockwise and counterclockwise circular components by the rotary spectral analysis technique (Emery and Thomson 2004). This technique has proven useful for the separation of highly circularly polarized motions, such as the inertial and tidal currents from mostly unidirectional seiche-driven currents having equal energy in both rotary components. Many of the rotary motion properties (among those clockwise and counterclockwise spectral energy components) are invariant under coordinate rotation so that local steering of currents by the bottom topography or the coastline does not influence the results of analysis.

To estimate the correlation between the current and wind velocity vectors a complex correlation coefficient $\rho = R\exp(i\Phi)$, introduced into physical oceanography by Kundu (1976), was used. Its magnitude $0 < R < 1$ measures the overall correlation of two series and the phase angle $\Phi$ displays the average counterclockwise angle of the current vector series with respect to the wind vector series. The phase angle is a quantity weighted according to the magnitude of the instantaneous vectors and it is more reliable when the magnitude of correlation is high.

For testing the steadiness of vector series a stability factor was calculated, which is a measure of the directional stability of the flow (current or wind). The stability factor (over a series) is calculated as a ratio of vector-mean and average-flow speeds multiplied by 100. The flow direction is constant if the value of the stability factor is 100.

Analysis of the rotary spectra of the raw data of the current and wind velocity revealed white noise at time scales shorter than 2 h. Therefore, the series were filtered by a low-pass Butterworth filter with 2-h cutoff to reduce measurement noise. The descriptive statistics was estimated from the filtered series. For the low-frequency analysis, the time series were filtered with a 36-h cutoff Butterworth filter and decimated to get hourly values. Such low-pass filtering almost removed various submesoscale oscillations, e.g. tidal and seiche-related currents, from the series.

## Results and discussion

### Basics of the wind and current

Highly variable, strong winds prevailed throughout the observation period (Fig. 2a) due to transit cyclones. The wind speed exceeded 10 m s⁻¹ during 60% and 15 m s⁻¹ during 16% of the whole period. Six strong wind events with the duration of about one day and with the speed exceeding 15 m s⁻¹ were recorded, including an extreme storm with the speed up to 24 m s⁻¹ on 23 November. In general, southerly winds prevailed and only three stronger wind events were mainly northerly.

The variability of the current velocity was basically similar to that of the wind velocity pattern (Fig. 2b). However, the current vector series were much more heterogeneous than the wind series, which resulted in a small correlation magnitude (0.47). A gradual vertical decrease of the mean current speeds from 16.9 ± 8.6 cm s⁻¹ to 12.4 ± 6.3 cm s⁻¹ was observed in the 1–5 m layer. During the strongest winds (23 Nov.) the current speeds in the upper bin reached up to 51 cm s⁻¹.
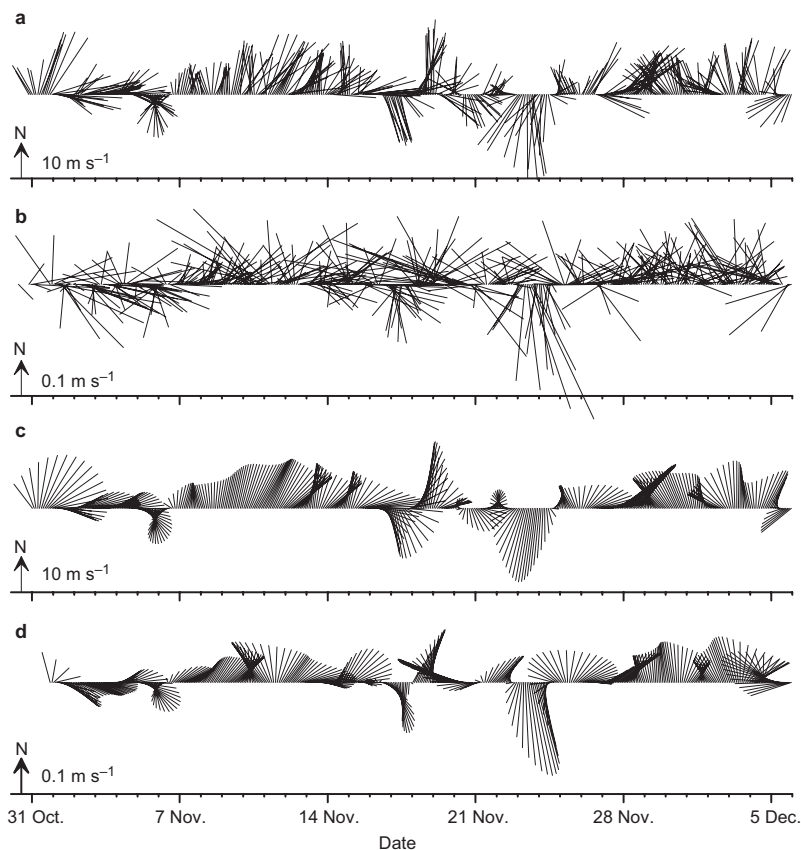
**Fig. 2**. Time series of (**a**, **c**) wind velocity and (**b**, **d**) current velocity vectors at 2.75 m depth subsampled over every 2 h. (**a**, **b**) filtered with a 2-h filter, (**c**, **d**) low-pass filtered with a 36-h filter. The scaling of vectors is shown by the northward directed arrow on the axes.

## Submesoscale oscillations of currents

Several significant energetic peaks with periods shorter than the typical transition time scale of atmospheric cyclones (1.5–2 days) were present in the wind spectra (Fig. 3a). Most of them reflected an anticyclonic character of motions and did not coincide with the most energetic peaks of current oscillations (Fig. 3b). As the spectra from all vertical bins were similar in shape, only the spectra from 2.75 m depth are shown. The peaks in the current velocity spectra in the period interval of 10–36 h probably indicate oscillations of the current due to seiches and tides. Seiches are a frequent phenomenon in the Baltic Sea, but there is still lack of observational data to determine the contribution of the exited currents. Tides are generally small with the tendency to increase towards the east in the Gulf of Finland and the corresponding currents are of the order of 1 cm s$^{-1}$ (Alenius *et al*. 1998 and references therein).

There is a distinct peak with a period at around 31 h in the wind and current spectra. In principle, this period of wind variations with about equal energy of rotary components (Fig. 3a) may reflect the response to small transient alternating cyclones and crests of anticyclones. The appropriate wind-driven currents could be expected to behave in the same manner and phase. However, our band-pass analysis showed definite bursts of oscillating currents on the temporal kinetic energy plots (Fig. 4a) with close connection to the strong wind fronts (rapid strengthening of wind and/or change of its direction) passing the site on 29 October and on 9, 15, 17/18 and 24 November (Fig. 5a). Therefore, we interpret them as seiche-related currents. The maximum current speeds during 31-h seiches ranged from 4 to 8 cm s$^{-1}$. Here, we note that these wind fronts excited all other seiches described below as well as inertial oscillations.

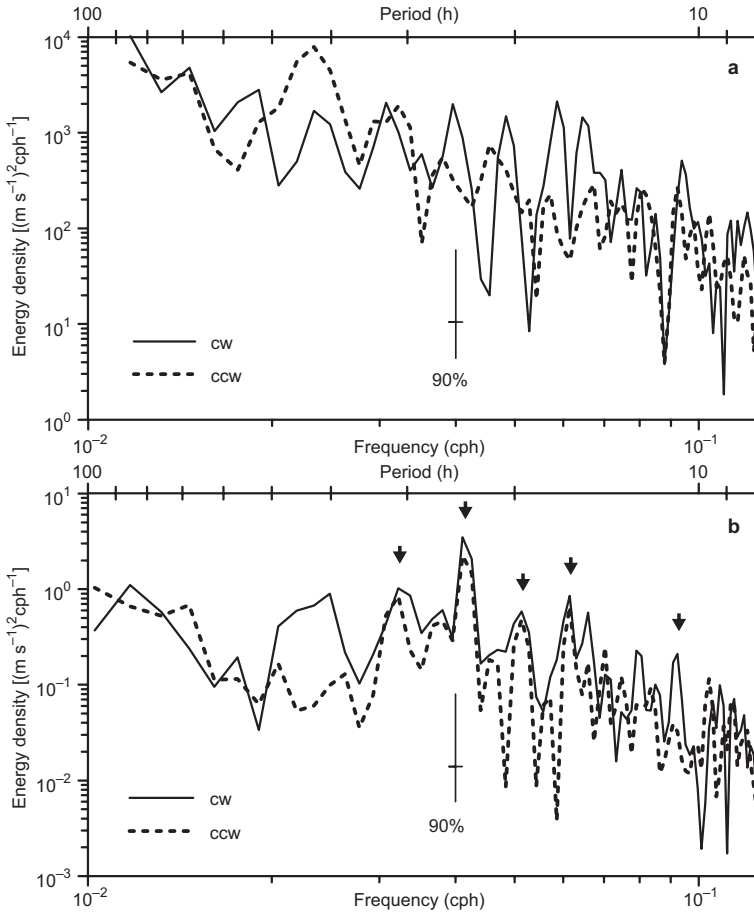The most prominent peak in the current spectra found at around 24 h corresponds well to

**Fig. 3**. Kinetic energy density spectra of (**a**) wind and (**b**) current at 2.75 m depth. Dashed line refers to the cyclonic spectrum (CCW: counterclockwise rotation), while solid line refers to the anticyclonic spectrum (CW: clockwise rotation). Vertical error bar shows the 90% confidence level. The arrows in **b** indicate seiche modes of 31, 24, 19.5, 16 and 11 h, respectively.
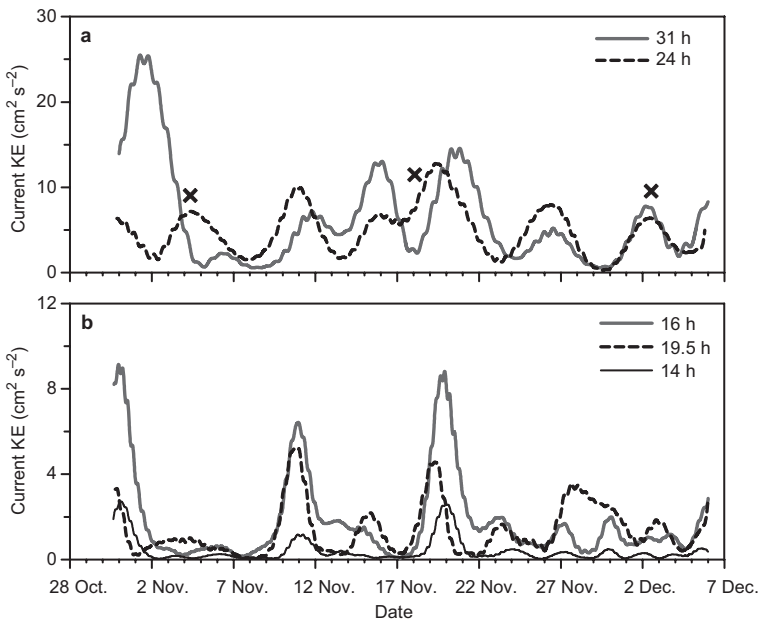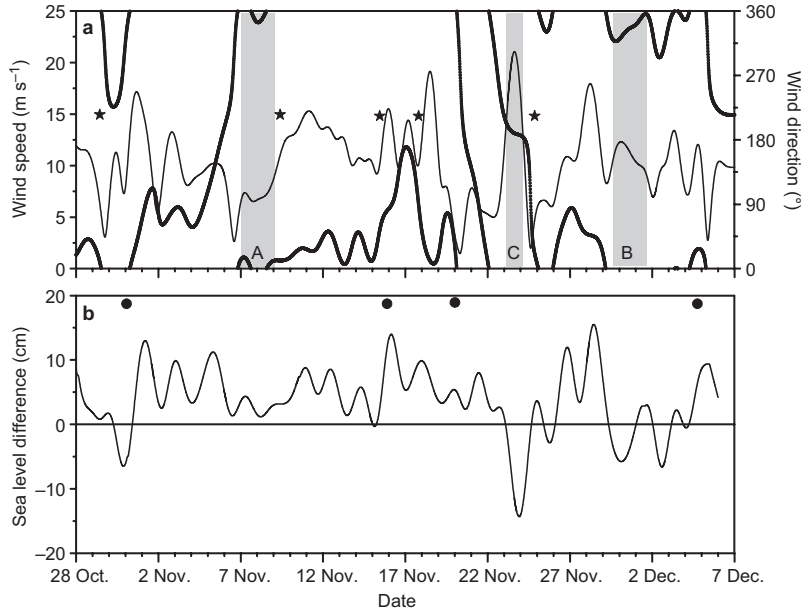


**Fig. 4**. Time series of band-pass current energy fitted by moving average (**a**) in 28.5–36 h interval corresponding to 31-h seiche mode and in 23–25 h interval corresponding to 24-h seiche mode and $K_1$ tidal constituent; (**b**) in 18.5–20.5 h interval representing 19.5-h seiche mode, in 15–17 h interval representing 16-h seiches' mode and in 13.5–14.5 h interval representing inertial oscillations. Crosses mark the timing of spring tide maxima.

**Fig. 5**. Time series of (**a**) wind speed (thin line) and direction (thick line), and (**b**) sea level difference between Sillamäe and Tallinn gauges. Shaded areas with the letters A, B and C in **a** designate steady wind periods and stars mark the timing of wind fronts that generated seiches. Dots in **b** indicate the timing when outflow pulses from Tallinn Bay occurred.

the $K_1$ diurnal tidal period (23.93 h). This suggests that a significant portion of a seiche-driven current with a period of ~24 h might be also involved. Actually, episodes of seiche oscillations with this period were present (Fig. 4a) and were characterized by the maximum current speed of about 5 cm s$^{-1}$. Diurnal tidal currents with maximum speeds up to 4 cm s$^{-1}$ were visible during 3 to 4 days after every 14 days, which points to their generation only during the spring tide. Note that the episodes of tidal currents on 4 November and 2 December occurred in the conditions of relatively weak winds (cf. Figs. 4a and 5a), but on 18 November the tidal episode coincided with a burst of a seiche-driven current and thus the kinetic energy was about doubled (Fig. 4a).

The spectral peaks, although less significant, found at around 19.5, 16 and 11 h (Fig. 3b) were evidently of seiche origin, which is seen on band-pass kinetic energy plots (Fig. 4b). Also, an almost equal peak value of clockwise and counter-clockwise spectra except for the 11-h period is characteristic of seiche-driven currents. The greatest current speed of 5 cm s$^{-1}$ was estimated for 16-h seiches. The duration of the episodes of inertial oscillations (local inertial period 13.9 h) was about 2 days (Fig. 4b) and the current speeds did not exceed 2 cm s$^{-1}$. We explain the weakness of inertial currents by very

shallow vertically unstratified water at the site. The amplitudes of semidiurnal tide constituents ($S_2$ and $M_2$) are considerably smaller than the ones of the diurnal tide ($K_1$ and $O_1$) in the Gulf of Finland as manifested by the sea level spectra (Johansson *et al.* 2001, Jönsson *et al.* 2008). This was supported also by our data showing relatively small current energy within the band of 11.5–13 h periods (Table 1).

Thus, our current velocity data and spectra revealed clearly seiche-driven currents with periods of the (most) energetic peaks for 31, 24, 19.5, 16 and 11 h. These period values are approximate due to the available resolution of the spectra from ±1.4 (31 h) to ±0.2 h (11 h). The duration of the oscillation bursts was 4–5 days depending on their intensity, while damping lasted 2 to 3 days and the maximum current speeds were in the range of 3–8 cm s$^{-1}$. The seiche-driven currents contributed about 15% to the total kinetic energy of currents (Table 1). This percentage is slightly overestimated due to entrained diurnal tidal currents. The periods of oscillations generally match the periods obtained from model simulations. The frequently cited study by Wübber and Krauss (1979), where the Coriolis force is included into the 2D-model of the Baltic Sea encompassing the Gulf of Finland, indicated seven oscillation modes with the

**Table 1**. Characteristics of band-pass current kinetic energy with explanation of involved processes.

| Band of periods (h) | Peak period (h) | Explained energy (%) | Processes involved |
|---|---|---|---|
| 4–10 | – | 4.5 | high-frequency currents |
| 10.5–11.5 | 11 | 0.3 | seiches |
| 11.5–13 | 12 | 0.9 | tides $S_2$, $M_2$ |
| 13.5–14.5 | 13.9 | 0.4 | inertial oscillations |
| 15–17 | 16 | 1.8 | seiches |
| 18.5–20.5 | 19.5 | 1.3 | seiches |
| 23–25 | 24 | 2.1 | seiches, tide $K_1$ |
| 25.25–28.5 | 26.5 | 3.7 | seiches, tide $O_1$ |
| 28.5–36 | 31 | 6.4 | seiches |
| > 36 | – | 74.9 | low-frequency currents |

periods exceeding 10 h. The periods of the first (31.0 h), fourth (19.8 h) and seventh (10.5 h) modes are very close to the periods estimated from our spectra. We point also to a weak energy peak at around 26.5 h (Fig. 3b), consistent with the second mode (26.4 h) of the model. In the recent study by Jönsson *et al*. (2008), the idea of the Baltic Sea oscillations as an ensemble of weakly coupled local (particular bay or sub-basin) oscillatory modes was proposed. Their model simulations showed two strongest oscillatory modes with periods of 27 and 23 h in the

Gulf of Finland, which are well comparable to the second (26.4 h) and third (22.4 h) oscillation modes of the model by Wübber and Krauss (1979). In fact, the seiche-driven current with the 24-h period in our data is also within the boundaries of the 23-h peak of this model (Jönsson *et al*. 2008: fig. 5). The significant oscillations with the 16-h period in the current velocity spectra have no references in the literature. Most likely they reflect the local seiches in Tallinn Bay.

## Wind and current relationship

The wind and current spectra were relatively similar in the low-frequency part with a considerable amount of energy between the periods of 40 and 50 h (Fig. 3). The wind variations with these periods and the dominance of the counterclockwise motion reflect typical transit cyclones at Baltic latitudes. Conversely, the currents responding to such wind conditions appeared to have anticyclonic character. Similar rotary spectral estimates from the northern Baltic Proper for the fall season were obtained by Nerheim (2004).

To study currents without the contribution of oscillating ones (described in the previous section) a low-pass filter with a cutoff period of 36 h was used. About 75% of the current variability remained as a result of this procedure (Table 1). The low-pass wind and current vector series over the whole observation period had generally a similar pattern (cf. Fig. 2c and d) with fairly good correlation (0.66–0.69) between them (Table 2), which supposedly is slightly underestimated due to the relatively large distance between the wind and current measurement sites. Nevertheless, such

**Table 2**. Statistical parameters of low-pass filtered current and wind velocity at different depth intervals. $U_c$ and $U_w$ are average current and wind speed with standard deviation. $R$ is the magnitude of the complex correlation coefficient between wind and current vectors. $\Phi$ is the average angular displacement of current vector with respect to the wind vector. All current velocity parameters were calculated as averages of two adjacent bins.

| Depth (m) | 1.5 | 2.5 | 3.5 | 4.5 |
|---|---|---|---|---|
| **whole period**: 30 Oct.–6 Dec. $U_w = 10.3 \pm 3.7$ m s$^{-1}$ | | | | |
| $U_c$ (cm s$^{-1}$) | 11.7 ± 5.1 | 10.1 ± 4.4 | 9.3 ± 4.1 | 8.6 ± 3.7 |
| $R$ | 0.69 | 0.66 | 0.66 | 0.66 |
| $\Phi$ (°) | 3 | 3 | 4 | 5 |
| **period A**: 7/8 Nov. (48 h) $U_w = 6.7 \pm 0.7$ m s$^{-1}$ | | | | |
| $U_c$ (cm s$^{-1}$) | 8.6 ± 1.2 | 7.8 ± 0.8 | 6.8 ± 0.7 | 6.8 ± 0.7 |
| $R$ | 0.77 | 0.73 | 0.76 | 0.80 |
| $\Phi$ (°) | 35 | 30 | 27 | 23 |
| **period B**: 29 Nov.–1 Dec. (48 h) $U_w = 11.1 \pm 0.9$ m s$^{-1}$ | | | | |
| $U_c$ (cm s$^{-1}$) | 10.2 ± 1.3 | 9.9 ± 1.3 | 9.9 ± 1.6 | 9.6 ± 1.6 |
| $R$ | 0.88 | 0.86 | 0.87 | 0.84 |
| $\Phi$ (°) | 34 | 37 | 36 | 34 |
| **period C**: 23/24 Nov. (24 h) $U_w = 18.5 \pm 2.2$ m s$^{-1}$ | | | | |
| $U_c$ (cm s$^{-1}$) | 24.2 ± 4.5 | 22.7 ± 4.1 | 21.6 ± 3.9 | 20.5 ± 3.7 |
| $R$ | 0.89 | 0.91 | 0.91 | 0.90 |
| $\Phi$ (°) | –5 | –6 | –5 | –4 |

magnitudes of correlation show that only about a half of the current variability at our site can be explained as 'wind-driven'. Considering that the observation period was five weeks, a variety of low-frequency constituents might be involved in the current velocity series. These background currents are usually due to the geostrophic pressure gradients. For a rough test of substantial buoyancy gradients we used the ADCP's temperature data. As characteristic of late fall, the water temperature gradually decreased from 10.1 to 6.4 °C over the observation period, but no anomalous water with temperature changes greater than 0.3 °C was observed (not shown). Therefore, we can leave out the currents related to the coastal mesoscale processes (e.g. upwelling, eddies), which commonly transport anomalous water. More likely, the general cyclonic geostrophic flow in the Gulf of Finland and the barotropic currents caused by the sea level adjustment due to winds, both topographically steered, mainly contributed to the pure wind-driven current. We will treat these aspects of the flow in the next section.

To study the strength of correlation and the rotation angle between the wind and current velocity vectors in more detail, we selected three periods (*see* Fig. 5a) when the wind and current were almost steady in speed (relatively low standard deviations, Table 2) and direction (stability factor values > 95). For comparison, the wind and current over the whole observation period were characterized by low stability factor values of about 50 and 35, respectively. Hereafter we denote these periods as A (7–8 Nov.), B (29 Nov.–1 Dec.) and C (23 Nov.). The first two, both lasting two days, represent situations with low and moderate wind speeds, respectively. Period C was chosen within an extreme storm on 23 November. The correlation between the wind and current within all selected periods was considerably stronger (up to ~0.9) as compared with that of the whole period (Table 2). As it followed from the lagged complex correlation coefficient, the wind led the current by 1–2 h for all analyzed observation periods. The current speed was highest at the surface and decreased continuously toward the bottom within all selected periods, but with the highest rate of ~1 cm s$^{-1}$ m$^{-1}$ during the extreme storm (Table 2). The average ratio of the near-surface current and wind speeds was

also the largest (1.35%) during this storm.

The near-surface current vector was rotated to the right from the wind vector except for period C (Table 2), which will be discussed in the next section. During periods A and B, the rotation angles at the depth nearest to the surface were 35° and 34°, respectively; i.e. almost independent on the wind speed (Table 2), and in accordance with many other similar observations (Lewis and Belcher 2004). An evident surface-to-bottom decrease of the rotation angle from 35° to 23° (veering of the current vector to the left) in the 4-m layer occurred when the wind was relatively weak (period A). Other periods with much stronger winds showed no significant vertical change of the veering direction. Such peculiar veering of the current vector during period A is not consistent with the Ekman model in the shallow sea, which predicts almost negligible clockwise veering. However, similar counterclockwise surface-to-bottom veering of the current vector was reported in the inner shelf off New Jersey (depth ~20 m) and was hypothesized as a veering contributed by a fluctuating alongshore density gradient through the thermal wind relation (Münchow and Chant 2000). In our case, i.e. under the conditions of a relatively low wind and very shallow unstratified sea, probably the moderate sea level adjustment due to earlier stronger westerly winds (Fig. 5a) controlled the flow. The current vector spirals in other shallow seas with depths of about 15 m (Lass *et al.* 2001, Cosoli *et al.* 2008) exposed the presence of both surface and bottom Ekman layers with different veering direction. Such obvious layering resulted explicitly from the pronounced vertical stratification during these studies.

Finally, we point to an important aspect (beyond the scope of the present study) of the wind and near-surface current relationship, which may refine the analysis. When the geostrophic flow and oscillatory currents are absent, the effects of wind are the main forcing mechanisms of the near-surface local currents. The momentum transfer from wind into the sea occurs through the wind shear stress and wave generation. Accordingly, the Ekman drift current and Stokes drift are induced, whereby dependently on the wave field parameters/state and fetch conditions the latter may be substantial (e.g., Mao and Heron
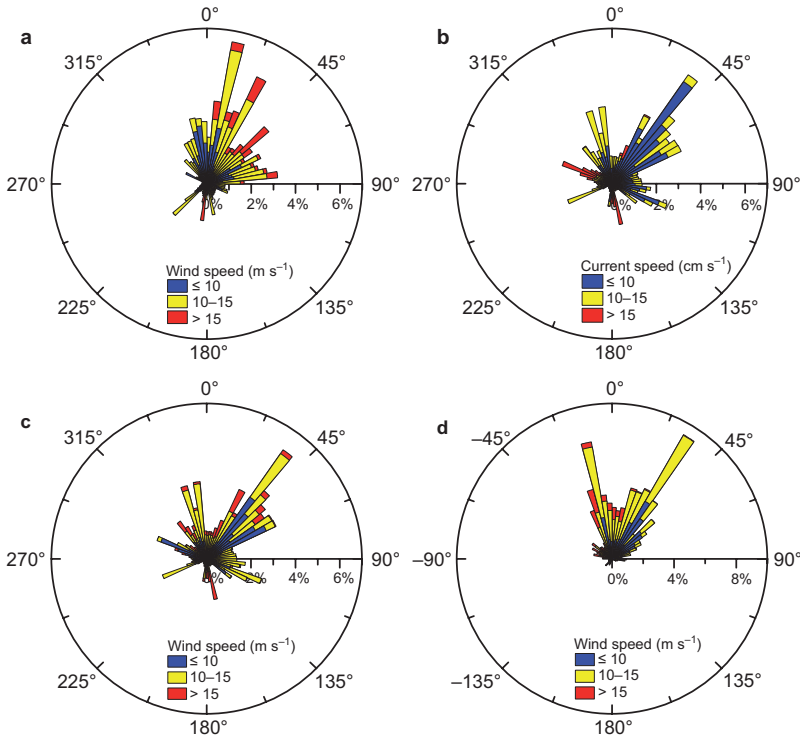
**Fig. 6**. Polar histograms of (**a**) wind direction with scaled wind speed, (**b**) current direction with scaled current speed, (**c**) current direction with scaled wind speed, and (**d**) rotation angle of the current vector with respect to the wind vector with scaled wind speed.

2008). Therefore, the measured Eulerian current velocities (at a fixed location) are actually a combination of the pure Ekman current and the current components caused by the Stokes-Coriolis forcing, i.e. a Stokes component and an Ekman-Stokes component (Polton *et al*. 2005). It is the latter that may be important as it attenuates over the whole surface Ekman layer, and thus may mask the speed and direction of the wind-driven Ekman current. The waves over our measurement site were presumably essential because the strong winds may cause enhanced wave heights over the banks as was shown by the wave model of Tallinn Bay (Soomere 2005: fig. 3).

## Effect of bottom topography on the current

There were evident indications in our data that the bottom topography in the vicinity of the site substantially affected low-frequency currents. Comparison of the directional distributions of the wind and the current velocity revealed several differences. The wind was predominantly

southerly and only a few short-duration northerly wind events occurred (Fig. 6a). In contrast, the directional distribution of the current was much more heterogeneous (Fig. 6b). A considerable number of current vectors lying in the directional sector of 25°–60° were veered ~30° to the right from the dominant wind direction and thus reflect the direct response to the wind. In addition, two clearly distinguishable relatively narrow bands of current directions with accompanying bands in the opposite direction, centered at about 295°/115° and 345°/165°, evidently point to a topographically steered flow. These steered currents were present during 24% of the whole observation period.

We related the band of current directions (295°/115°) to the flow at the southern border of the channel between Uusmadal and Naissaar banks (Fig. 1). This direction of currents fits well with the along-channel direction. The eastward (115°) flow was characterized by moderate current speeds (Fig. 6b) and took place as a single event on 1–3 November when the westerly wind was relatively strong (Figs. 5a and 6c). Therefore, this inflow channeled into Tallinn Bay, was

probably produced by an uncommon (within our observation period) favorable westerly wind event. The westward outflow (295°) from Tallinn Bay through the channel with a relatively high speed of > 15 cm s⁻¹ (Fig. 6b) occurred during weaker winds (Fig. 6c). Altogether four outflow pulses with a duration of about one day were observed and these were mostly related to the maxima of the sea level differences between Sillamäe and Tallinn (Fig. 5b). A similar correlation of low-frequency current with sea level difference was earlier observed in the Irbe Strait (Lilover *et al*. 1998). The flow along the second band of current directions (345°/165°) explicitly occurred when the wind speed was high or extreme (Fig. 6c). The northward (345°) current speeds were moderate (mainly 10–15 cm s⁻¹), but the southward (165°) ones, representing mainly an extreme storm situation on 23 November, were much stronger (Table 2). Note that the directions of these currents were nearly parallel to the major axis of Naissaar Bank (Fig. 1).

Thus, the topographically steered currents have their specific directions, which are independent of wind direction. That is why the distribution of the rotation angles of the current vectors with respect to the wind vectors had two pronounced maxima at the rotation angles of about 35° and –15° (Fig. 6d). The former with its surrounding rotation angles indicates the 'normal' wind-driven currents during weak or moderate winds. The latter dominant band consisted of negative rotation angles meaning that the current was directed to the left from the wind vector and therefore reflected a topographic effect. We mention here that coincidence of the maximum of the counterclockwise rotation angle (–15°) and the direction of topographically steered currents (345°/165°) during very strong winds is occasional and is due to our data set. The distribution of rotation angles reveals also that the stronger the wind the more negative is the angle (Fig. 6d). The corresponding plot of rotation angles *versus* wind speeds indicates a fairly good relationship despite some scatter of points (Fig. 7). The fitted linear regression line intersects the zero rotation angle at the wind speed of 12.5 m s⁻¹. In other words, this wind speed value roughly determines the threshold of switching between the wind-driven current and the topographically steered current.
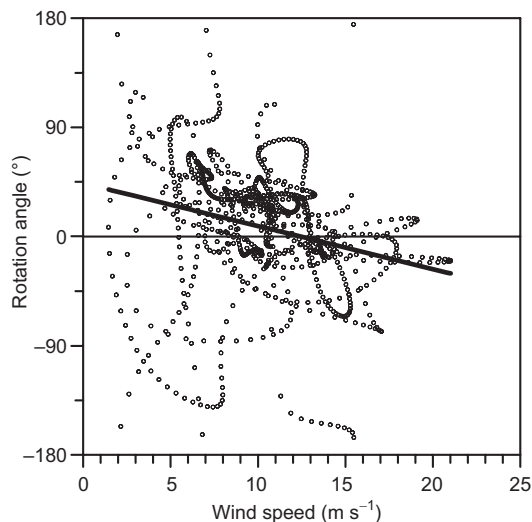


**Fig. 7**. Scatter-plot of the rotation angle of the current vector with respect to the wind vector and wind speed. The line is the least-squares fit.

## Conclusions

The observed variations of currents generally had a pattern coinciding with that of the variable wind. The low-frequency currents (in time scale > 36 h) contributed 75% and different oscillating currents ~15% to the total energy of currents. Nearly 50% of the overall low-frequency current variations were found to be wind-driven, but during shorter periods of steady wind and current the role of wind rose up to 75%. Because of the complicated bottom topography around the site about 25% of the low-frequency currents were evidently steered.

The strong wind fronts generated seiches and corresponding current oscillations as well as very weak inertial oscillations. The most energetic seiche-driven oscillations were found at periods of 31, 24, 19.5, 16 and 11 h and they appeared as bursts with durations of 4–5 days and maximum current speeds of 3–8 cm s⁻¹. Tidal current oscillations (dominantly $K_1$ constituent) were observed only during the spring tide.

The response of the low-frequency current to the steady wind forcing was in a reasonable accordance with the Ekman model for the very shallow sea. It follows from a slight gradual surface-to-bottom decrease of the current speed and the rotation of the current vector to the right from

the wind vector by 35°. In an exceptional case, a significant surface-to-bottom counterclockwise veering of the current vector was probably caused by the barotropic flow component due to the sea level gradient along Tallinn Bay.

At times the currents were topographically steered along either of the two dominant directions. First, during very strong winds the flow was definitely aligned parallel to the major axis of Naissaar Bank. Second, the outflow pulses from Tallinn Bay through the 'channel' between Naissaar Bank and Uusmadal Bank occurred during weaker winds and were obviously caused by the along-channel large sea level gradients.

To summarize, the presented analysis enabled us to resolve the nature of currents as a response to variable winds in a very shallow sea. An important topic for future studies will be estimation of the role of surface waves (Stokes drift), which may considerably mask the Eulerian current data.

# References

Alenius P., Myrberg K. & Nekrasov A. 1998. Physical oceanography of the Gulf of Finland: a review. *Boreal Env. Res.* 3: 97–125.

Andrejev O., Myrberg K., Alenius P. & Lundberg P.A. 2004. Mean circulation and water exchange in the Gulf of Finland — a study based on three-dimensional modelling. *Boreal Env. Res.* 9: 1–16.

Book J.W., Perkins H., Signell R.P. & Wimbush M. 2007. *The Adriatic Circulation Experiment winter 2002/2003 mooring data report: a case study in ADCP data processing*. Memo. Rep. NRL/MR/7330-07-8999, U.S. Naval Res. Lab., Stennis Space Center, Miss.

Cosoli S., Gačić M. & Mazzoldi A. 2008. Variability of currents in front of the Venice Lagoon, northern Adriatic Sea. *Ann. Geophys.* 26: 731–746.

Emery W.J. & Thomson R.E. 2004. *Data analysis methods in physical oceanography*. Elsevier, London.

Gästgifvars M., Lauri H., Sarkanen A., Myrberg K., Andrejev O. & Ambjörn C. 2006. Modelling surface drifting of buoys during a rapidly-moving weather front in the Gulf of Finland, Baltic Sea. *Estuarine Coast. Shelf Sci.* 70: 567–576.

Johannson M., Boman H., Kahma K.K. & Launiainen J. 2001. Trends in sea level variability in the Baltic Sea. *Boreal Env. Res.* 6: 159–179.

Jönsson B., Döös K., Nycander J. & Lundberg P. 2008. Standing waves in the Gulf of Finland and their relationship to the basin-wide Baltic seiches. *J. Geophys. Res.* 113: C03004, doi:10.1029/2006JC003862.

Kundu P.K. 1976. Ekman veering observed near the ocean bottom. *J. Phys. Oceanogr.* 6: 238–242.

Laanemets J., Pavelson J., Lips U. & Kononen K. 2005. Downwelling related mesoscale motions at the entrance to the Gulf of Finland: observations and diagnosis. *Oceanol. Hydrobiol. Studies* 34: 15–36.

Lass H.U., Mohrholz V. & Seifert T. 2001. On the dynamics of the Pomeranian Bight. *Cont. Shelf Res.* 21: 1237–1261.

Launiainen J. & Laurila T. 1984. Marine wind characteristics in the northern Baltic Sea. *Finnish Mar. Res.* 250: 52–86.

Lentz S.J., Fewings M., Howd P., Fredericks J. & Hathaway K. 2008. Observations and model of undertow over inner continental shelf. *J. Phys. Oceanogr.* 38: 2341–2357.

Lewis D.M. & Belcher S.E. 2004. Time-dependent, coupled, Ekman boundary layer solutions incorporating Stokes drift. *Dyn. Atmos. Oceans* 37: 313–351.

Lilover M.J., Lips U., Laanearu J. & Liljebladh B. 1998. Flow regime in the Irbe Strait. *Aquat. Sci.* 60: 253–265.

Mao Y. & Heron M.L. 2008. The influence of fetch on the response of surface currents to wind studied by HF ocean surface radar. *J. Phys. Oceanogr.* 38: 1107–1121.

Münchow A. & Chant R.J. 2000. Kinematics of inner shelf motions during the summer stratified season off New Jersey. *J. Phys. Oceanogr.* 30: 247–268.

Nerheim S. 2004. Shear-generating motions at various length scales and frequencies in the Baltic Sea — an attempt to narrow down the problem of horizontal dispersion. *Oceanologia* 46: 477–503.

Polton J.A., Lewis D.M. & Belcher S.E. 2005. The role of wave-induced Coriolis-Stokes forcing on the wind-driven mixed layer. *J. Phys. Oceanogr.* 35: 444–457.

Raudsepp U. 1998. Current dynamics of estuarine circulation in the lateral boundary layer. *Estuarine Coast. Shelf Sci.* 47: 715–730.

Soomere T. 2005. Wind wave statistics in Tallinn Bay. *Boreal Env. Res.* 10: 103–118.

Suursaar Ü. & Aps R. 2007. Spatio-temporal variations in hydro-physical and -chemical parameters during a major upwelling event off the southern coast of the Gulf of Finland in summer 2006. *Oceanologia* 49: 209–228.

Talpsepp L., Nõges T., Raid T. & Kõuts T. 1994. Hydrophysical and hydrobiological processes in the Gulf of Finland in summer 1987: characterization and relationship. *Cont. Shelf Res.* 14: 749–763.

Wübber C. & Krauss W. 1979. The two-dimensional seiches of the Baltic Sea. *Oceanol. Acta* 2: 435–446.

Zhurbas V., Laanemets J. & Vahtera E. 2008. Modeling of the mesoscale structure of coupled upwelling/downwelling events and the related input of nutrients to the upper mixed layer in the Gulf of Finland, Baltic Sea. *J. Geophys. Res.* 113: C05004, doi: 10.1029/2007JC004280.